CONF-880772--2

DE89 005802

Overview of the ANL Advanced LMR System Thermal-Hydraulic Test Program Supporting Both GE/PRISM and RI/SAFR

by
J. J. Oras, T. M. Kuzay, and K. E. Kasza
Argonne National Laboratory
Materials & Components Technology Division
9700 S. Cass Avenue, Bldg. 308
Argonne, IL 60439

1. Abstract

Descriptions of the ANL thermal-hydraulic water models of both the PRISM and SAFR reactors are presented, together with results from Phases I and II of the thermal-hydraulic test program. Phenomena discovered during these tests and modeling results are presented. Overall, these efforts demonstrate the acceptable thermal-hydraulic performance of both the PRISM and SAFR concepts.

2. Introduction

In 1985, the Argonne National Laboratory (ANL) initiated a water test program utilizing its Mixing Components Test Facility (MCTF) to support the needs of the Advanced Liquid Metal Reactor (ALMR) program for development of inherently safe and cost-competitive reactors. A test program was developed jointly between ANL and GE Nuclear Energy in support of the PRISM concept[1] and between ANL and RI in support of the SAFR concept. The broadly stated objectives of this program are to use the MCTF for transient and steady-state thermal-hydraulic water flow tests to explore important high- and low-flow natural convection operation scenarios for assessing factors influencing thermal-hydraulic performance, reactor coolability, and structural thermal distributions.

Complete geometric models were built because the thermal-hydraulic performance of one subregion of the prototype under a variety of conditions will depend upon the conditions prevailing elsewhere in the reactor. Besides geometric similitude, both Richardson number (the ratio of buoyancy to inertia forces) and Euler number (the ratio of pressure to inertia forces) similitude were maintained during testing.

Both the Phase I and Phase II tests of a multiphase program aimed at establishing the reliability and inherent safety of both advanced reactor design have been completed. This paper describes both the PRISM and SAFR test models and presents test results obtained during the first two phases of the program.

3. Background

A. Modelling Laws

A non-dimensionalization of the governing one-dimensional conservation equations for a flow field yields a number of similarity

DISCLAIMER

parameters. Generally, complete similarity cannot be achieved for complex problems. Differences in materials of construction, e.g., plastic in the model versus steel in the prototype, introduces other obstacles to achieving complete similarity.

The modelling approach for the ANL models maintained Richardson and Euler number ratios equal to unity between the model and prototype. However, model and prototype similarity for the Euler number ratio could not be achieved over the entire flow range but was matched at about 10% prototype flow using resistance orificing in the model core and in the intermediate heat exchangers (IHXs).

The systematic consideration of the tradeoffs for various model designs and facility control constraints led to fixing the PRISM and SAFR model designs to geometric scales of 1/5.24 and 1/11.2 respectively of the prototype.

B. Model Description

The PRISM test model is shown schematically in Figure 1, and a picture of the completely assembled and instrumented SAFR test model is presented in Figure 2. Both models are constructed of transparent plastic materials. All major in-vessel components are represented except the active IHX heat sinks which were not available for the Phase I tests. The PRISM model fits in a two-piece, cylindrical 1.06-m (41.8 in.) inner diameter by 2.90-m (114 in.) tall steel vessel with large transparent windows for laser flow visualization. The SAFR model fits in the lower half of this same pressure vessel. The reactor core is simulated by a 60 KW electrical-resistance immersion heater with computer-interfaceable power control.

Computer-controlled forced flow is provided in two ways: for low-flow conditions, (less than 10%) in-vessel pumps (propellers driven by 0.25-hp dc motors with SCR controllers) are used; for high-flow conditions, the MCTF water loop is used as explained later. Computer control of the immersion heater and pumps allows transient simulations. Heat sinks were installed in the IHXs for the Phase II testing.

Referring to Figure 1, water flows up vertically in the 0.44-m (17.5-in.) inner diameter core barrel over the immersion heater elements, through the core resistance simulater, and into the upper plenum. From the upper plenum the water normally flows into the two IHX inlets and proceeds downward where it empties via two exit pipes per IHX into the annular region between the radial shield and the containment vessel wall. It continues downward through this region until it turns radially inward just below the radial shield, where it is drawn upwards through the radial shield into four pump inlets. The flow leaves the pump exit plena in the downward direction by means of eight core inlet pipes (four pipes per pump exit plenum) to return either to the core or, by way of two exit manifolds, to the MCTF depending on the mode of operation.

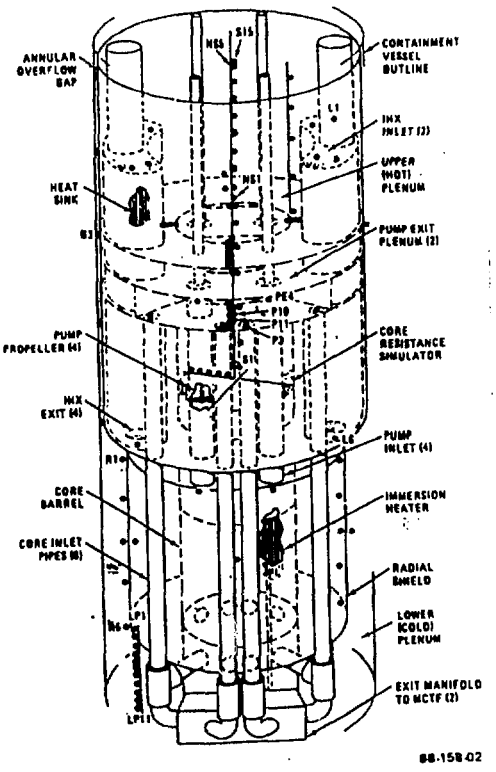

Fig. 1. Thermal hydraulic model of the PRISM advanced liquid metal reactor concept.

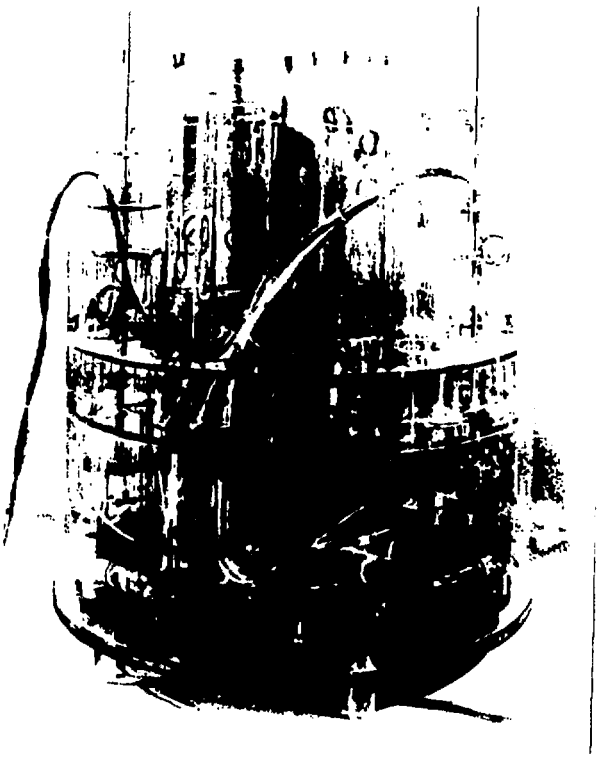

Fig. 2. Thermal hydraulic model of the SAFR advanced liquid metal reactor concept.

Included in the model is a 0.0064-m annular overflow gap for the study of transients involving RVACS cooling. Perforated plates are located at the IHX inlets and outlets and the core exits to provide the proper pressure drops through these flow paths respectively.

In the SAFR model, referring to Figure 2, water flows up vertically in the 17-1/2 in.-ID core barrel over the immersion heater elements, through the core resistance simulator, and into the hot plenum. From the upper plenum it flows into the four IHX inlets and proceeds downward where it empties via the exit pipes from IHXs into the cold plenum. From the cold plenum it is drawn upwards into two pump inlets. The flow leaves the pump exit plena in the downward direction by means of eight core inlet pipes (four pipes per pump exit plenum) to return either to the core or, by way of the exit manifolds, to the MCTF, depending on the mode of operation. Included in the model is a 1/4 in. (in Phase I, the annular gap was 0.125 in.) annular overflow gap for the study of transients involving RVACs cooling. A stack of perforated plates provide the proper pressure drop through the core at the core exit.

Near the bottom of the models in the core barrel, an inner tube serves as flow diverter. This inner tube, when inflated, blocks off

the flow from the eight core inlet pipes and thus allows the flow to be routed back to the MCTF. Outside the core barrel, ducting connects the core inlet pipes to the exit manifolds and the MCTF.

Thermocouples are positioned at the entrance and exit of each subregion as indicated in Figures 1 and 2. Thermocouples mounted on vertical stings* are used to measure radial or circumferential temperature gradients in key regions.

Pressure taps are located at the entrance and exit of key subregions. These pressure taps can be used to inject dye to make time-of-flight measurements and thus, to determine velocities in key regions.

The heat sinks in the IHXs consist of copper coils packed inside the IHX shells through which cooling water is circulated. Test results indicated that the heat sink capability was about 69 kW for PRISM which is 25% of model full power, and 52 kW for SAFR which is 19% of model full power.

C. Test Program

The Phase I tests facilitated the shakedown process and the development of control features and subsystems which have been incorporated in the test models. These tests also highlighted specific thermal-hydraulic phenomena of potential interest to designers. A series of 18 tests in PRISM and SAFR Phase I testing were conducted in the following general categories: (1) isothermal flow distribution, (2) hot plenum free-surface behavior, (3) constant-flow thermal transients, (4) hot plenum free-surface behavior, and (5) mixed forced/natural-convection flows.

A total of 20 tests were conducted during Phase II of the PRISM test program. These represented five prototypic duty cycle transients chosen because of their severity or frequency of occurrence. The transients simulated were: (1) Plant unloading at 3% per minute from 100 to 25% power (Event A-4), (2) Reactor trip from full power with maximum decay heat (Event B-1A), (3) Loss of power to one primary pump (Event B-3B), (4) Loss of feedwater to all modules supplying one turbine with scram after steam generator dryout (Event B-5B), and (5) Loss of feedwater to all modules supplying one turbine with 30 second delayed scram (Event B-5B).

For SAFR in Phase I, the following prototypic transient tests were conducted: (1) B-02 type, cold shock to the hot plenum, (2) C-05 type, severel cold shock to the hot plenum, (3) B-13 type, hot shock to the cold plenum, and (4) N-1 loop asymmetric flow operation when one pump is alternatively shut down while the two IHXs are rendered inoperational (plugged).

---

*Stings of thermocouples are used here to denote thermocouples mounted in a straight line.

In Phase II of SAFR, after installation of the heat sinks in the IHXs, similar generic and feature tests in the previous Phase I testing were repeated. The ALMR program was redirected before any of the RI-defined, sophisticated Phase II transients could be tested.

4. Test Results

A. PRISM

Summary results from all tests are presented followed by more detailed discussions of the cold pool stratification phenomena observed during the Phase I constant flow thermal transient test series and the reactor trip test from the Phase II tests. Results from the tests support the acceptable thermal hydraulic performance of PRISM ALMR concept.

a. Constant Flow Thermal Transients

Under isothermal constant-flow conditions at 10% or less of simulated prototype flow, a stagnant recirculation region was observed in the bottom of the lower plenum while the region above was well mixed. At higher flowrates all regions of the lower plenum and in the upper plenum were well mixed.

A series of four tests were run with 5, 15, 30, and 60% of simulated prototype full flow supplied by the MCTF and with a nominal up-ramp in temperature of 16.7C (30F) for all tests. The Richardson and Reynolds numbers based on core barrel ID for these tests ranged from 21 to 3021 and 1434 to 16392, respectively. The results of test JU1901 with 15% of simulated prototype full flow will be highlighted, and comparisons will be made with the remaining tests. The flowrate and temperature of the water at the core inlet remained constant from 40s until the end of the test at 5500s.

The responses of thermocouples mounted on a vertical sting (Fig. 1) on the cold plenum floor about 0.051-m inside the radial-shield liner are shown in Fig. 3. LP1 is located approximately 0.051-m above the bottom edge of the radial-shield liner and LP11 is located 0.054-m above the floor of the cold plenum. The results in Fig. 3 show that there is a time delay of 500s before hot fluid reaches the thermocouple sting. Dye was also inject at the exits of an IHX and the thermally stratified dyed interface was measured 0.286-m above the cold plenum floor whereas the bottom edge of the radial-shield liner is 0.320-m above the plenum floor. The cold stagnant region below the stratified interface is clearly indicated in Fig. 3 and begins forming at 500s. Thermocouples LP1 through 3 are above the interface elevation.

The stratified interface was observed at approximately the same elevation by means of dye injection in the tests with 5, 30, and 60% flow rates. The interface for the 60% flow test was not as distinct indicating some turbulent mixing and it moved down toward the plenum floor more rapidly. In contrast, the interface was extremely distinct and motionless and appeared as a fine line in the 5% flow test.

However, the cold stagnant region formed at flowrates greater than 10% because of the strong thermal buoyancy forces which oppose the downward-acting inertia forces of the fluid. The lower plenum above the stratification interface as well as the upper plenum were well mixed at all flow rates.

The response of thermocouple G3 at mid-elevation in the overflow gap surrounding the hot plenum was nonlinear which is an indication of heat transfer by convection as well as conduction. The existence of natural convection currents in the gap will enhance heat removal by the RVACS under conditions were there is no overflow through the gap.

The hot upper plenum was found to be well mixed in all tests with essentially no stratification. Unlike in the cold lower plenum, the thermal-buoyancy and inertial forces act in the same direction and thus do not promote stratification. The cold fluid initially in the upper plenum mixes with the core flow and is washed out of the upper plenum.

Response for a vertical sting of thermocouples mounted on the outer surface of the radial-shield liner in the cold pool are presented in Fig. 4. The responses generally fall on top of one another if the initial thermocouple offsets are factored in. This behavior is evident in all four tests and indicates the absence of stratification in that portion of the cold pool that is in the flow path to the core.

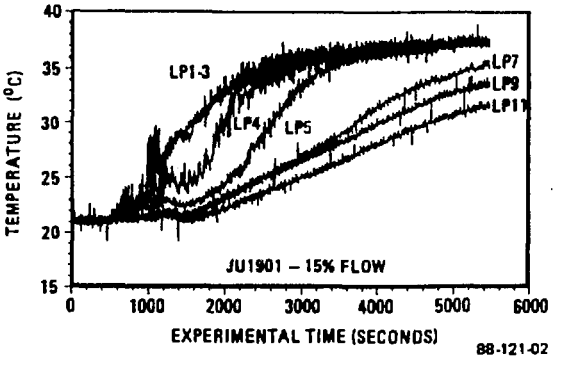

Fig. 3. Development of thermal stratification in the model cold plenum during a constant-flow thermal-upramp transient.

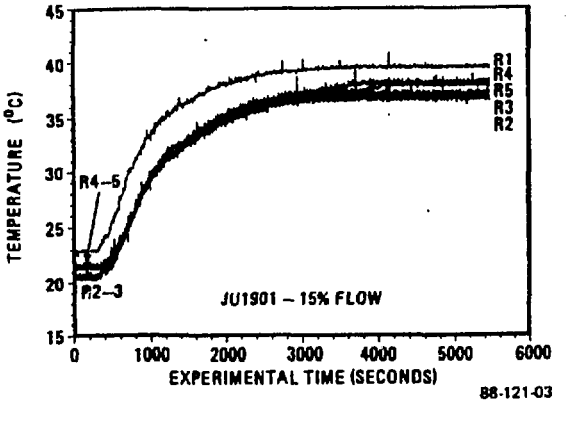

Fig. 4. Vertical variation of model flow temperature on the outside of the radial shield for a thermal-upramp transient.

b. Reactor Trip Transient

Tests simulating the GE prototype transient B-1A, reactor trip from full power with maximum decay heat, were conducted in the Phase II tests. Results with a core temperature difference of 8.1C (14.6F) are presented. Water flow was provided by the MCTF loop

during the initial portion of the transient. At 69s, the immersion heater was turned on while the flow was still provided by the MCTF loop. The MCTF was completely isolated from the model at approximately 420s and the transient continued with the immersion heater and internal pumps providing the power and flowrate, respectively.

The response of thermocouples mounted on the vertical sting on the cold plenum floor showed that the thermocouple responses fell on top of one another indicating that there was no stratification in the lower plenum. This was expected since the conditions necessary for stratification are not created with a cold shock to a cold plenum with the buoyancy and inertia forces acting in the same direction. Dye injected from the left exit of the left IHX immediately after transition to internal flow drifted predominantly downward and filled the lower plenum.

The responses of four thermocouples located in the upper plenum on the center sting are presented in Fig. 5. The plenum started out at a uniform temperature, and restratified after 1200s. This transient is a cold shock to a hot upper plenum, in which the buoyancy and inertia forces oppose each other. Under these conditions, stratification in the upper plenum can be expected if the buoyancy forces are large enough compared to the inertia forces. During the entire test, the flowrate and power were gradually decreasing and thus the relative strengths of the inertia forces and buoyancy forces were varying. This variation accounts for the complex phenomenon observed in Fig. 5. The gradual cooling of the model, observed after 1200s, is caused by a higher than nominal IHX heat sink capacity relative to the core heating.

Responses of the thermocouples mounted on the outer surface of the radial-shield liner indicated that there was essentially no stratification in the radial-shield gap region. Although slight stratification was exhibited in the thermocouple responses of R1 and R5 in the period between 300 and 900s, the degree of stratification present caused no loss of coolability to that region.

The responses of thermocouples located at the entrances and exits of critical subregions (refer to Fig. 1) are presented in Fig. 6. Generally, after 1800s, the model was stratified with a flowrate of less than 6% of full flow and was cooling down due to the greater heat sink capacity of the IHXs compared to the power provided by the immersion heater.

In summary, the simulation of transient B-1A indicates the existence of some stratification in the upper plenum for a short period of time, no stratification in the lower plenum, very small rates of change of temperature in internal structures, and generally favorable coolability of the entire model after the scram.

Reverse flow in the shutdown pump during transient B-3B, corresponding to the loss of power to one primary pump, was observed during portions of the transient as the relative strengths of the buoyancy and inertia forces changed. The consequences of the presence

of reverse flow in the shutdown pump has not been evaluated yet, but this transient is suggested as a potential candidate for simulation by COMMIX-1A as part of the code validation effort.

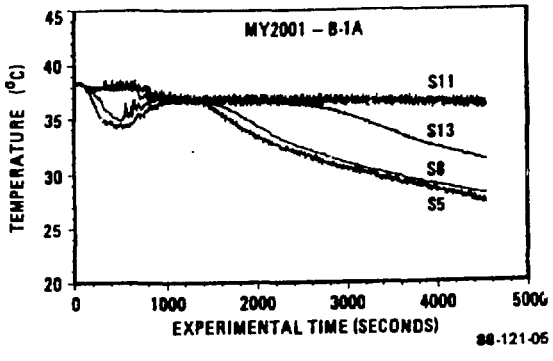

Fig. 5. Responses of thermocouples in the upper plenum at various elevations for the reactor trip transient.

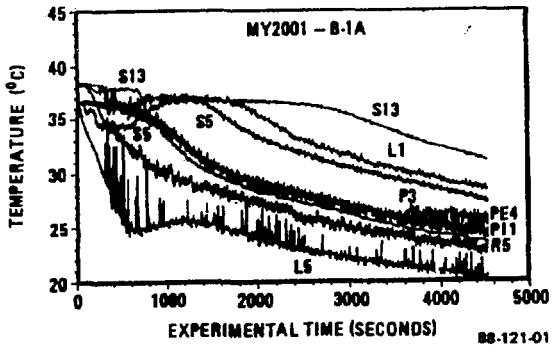

Fig. 6. Model temperature responses at the inlets and outlets of various subregions for the reactor trip transient.

B. SAFR

Summary results from all tests are presented followed by more detailed specific test data to highlight pool stratification and thermal asymmetry in SAFR. Results from the tests support the expected thermal hydraulic performance of SAFR ALMR concept.

Constant flow, thermal upramp tests with no heat removal capacity through the IHXs in Phase I resulted in severe thermal stratification in the cold plenum, even at 20% flow rate.

In these tests the hot plenum was observed to mix readily. In both plena, but specifically in the cold plenum. The geometric plane of symmetry provided with the design was also the symmetry plane for the thermal-hydraulic phenomena. The redon between the hot and cold pools did function as well as a thermal insulation zone between the hot and cold plena.

The non-transient type test results are confined to those obtained during Phase II. With the installation of heat sink capability in the IHXs, the results became more prototypic for the generic phenomena.

a. Mixed, Forced-Natural Convection Tests

Under isothermal constant-flow conditions at 10% or less of simulated prototype flow, a stagnant zone was observed in the bottom of the cold plenum. At higher flow rates both plena were well mixed. Flow distribution through the IHXs were uniform.

In 1-1/2 hr. heat-up and 1/2 hr. cool-down test, the core heater was set at 27.5 kw (10% full power level in the model) while the two internal pumps circulated the water at 11.5 gpm (17% of full flow in the model). This was the last of a set of discrete tests where the heater power was increased from 2.5% of full power in increments of 2.5% to 10% while the internal circulation level was fixed at the 11.5 gpm level.

No significant stratification was found in the hot plenum during Phase I testing. The design asymmetry of SAFR did not cause significant asymmetry in thermal-hydraulics in the hot plenum. The IHX bank side in Phase II testing accentuated any existing or forming thermal stratification whereas such stratification disappeared rapidly on the opposite side.

In the cold plenum, asymmetric thermal stratification was formed in these series of tests. For existing or forming thermal stratification in the cold plenum would linger persist longer on the pump side than on the side with the IHX bank).

In mixed, forced natural convection at constant flow core power and with heat removal through the IHXs, the hot plenum exhibited good mixing behavior overall. In the cold plenum, the 0-degree axis zone was found thermally more isolated than the 180-degree zone on the IHX bank side.

b. Natural Circulation Tests

The natural circulation tests were run at 6, 14.1, 20, and 27.5 KW core heater power levels ranging from 2 to 10% of the full power while the secondary side in IHXs were turned on to remove the heat.

Data and observations from all the tets were self-consistent, however, with increasing intensity as the core power became higher. Both the hot and the cold plena in SAFR exhibit strong thermal asymmetry under natural circulation. Natural circulation causes flow stratification in these plena. The hot plenum stratifies strongly on the 0-degree side; whereas the IHX bank remains nearly uniform in temperature at all elevations.

In the cold plenum the above trend is reversed. The stratification becomes very prominent on the 180-degree side; and the 0-degree side becomes uniform in temperature. This behavior is illustrated in Fig.s 7 and 8. The stratification in the cold plenum on the 0-degree side lasts up to 6000s after which it is mitigated.

c. Select Transient Tests

In light of the thermal asymmetry demonstrated in the previous tests, the asymmetric operation tests of Phase I are of interest. During these tests, unlike the previous ones, the heat removal capacity was not available. The two IHXs, #1 and 2, were plugged. The circulating pump was first chosen to be pump #1, in the opposite

half of the reactor vessel as the non-plugged IHXs. In another test, the circulating pump, pump #2, was in the same half of the vessel as the non-plugged IHXs. The model core power was set at 27.5 KW (10% of full power) while the single pump was circulating the flow at about 8% level of the full flow. Under these conditions, the hot plenum was uniform in temperature with no stratification. The cold plenum stratified very strongly. This is shown, in Fig. 9, with the vertical sting TC data at 180-degree position.

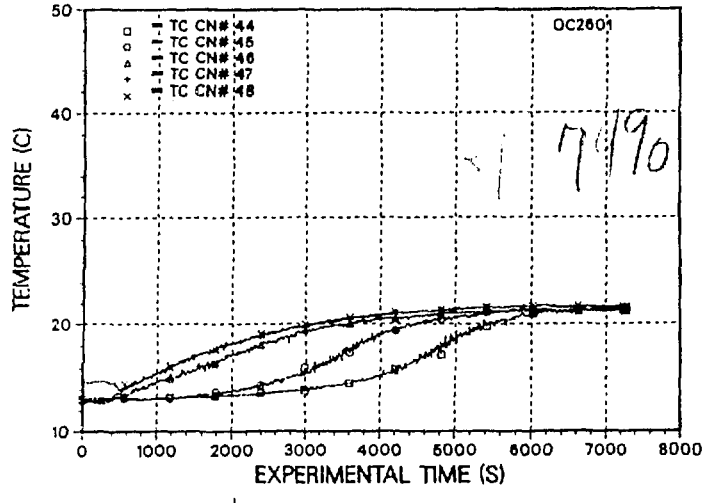

Fig. 7
Natural circulation test at 10% power. The cold plenum vertical sting TC data at 180-degree postion.

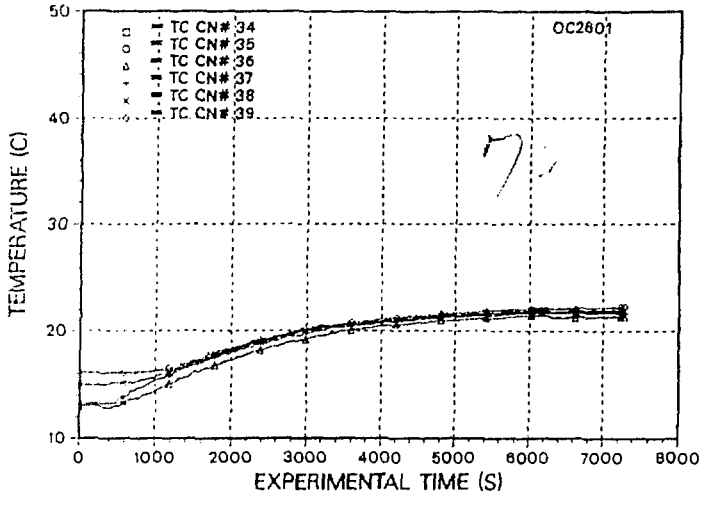

Fig. 8
Natural circulation test at 10% power. The cold plenum vertical sting TC data at 0-degree position.

The cold plenum data was almost identical to that shown in Fig. 9 when the operational pump was switched to be pump #2. However, this time the hot plenum, which has not stratified in the previous test, also showed significant initial stratification which was abated by 400s of the 1300s long test. This phenomena demonstrates that in SAFR when the operational elements (pump and IHXs) are confined to one-half of the vessel geometry preferrential thermal paths will occur.

In other transient such as cold shock to hot pool (B-02 and C-05) and hot shock to cold pool (B-13) severe thermal stratifications were observed to occur in the pool in question. In Fig. 10, the hot

plenum vertical sting TC data is shown at 0-degree position from C-05 test. The opposite one at 180-degree position shows very similar data. In this 30% pump ramp-down transient, the hot plenum goes through a severe cold shock and the cold plenum goes through a severe hot shock.

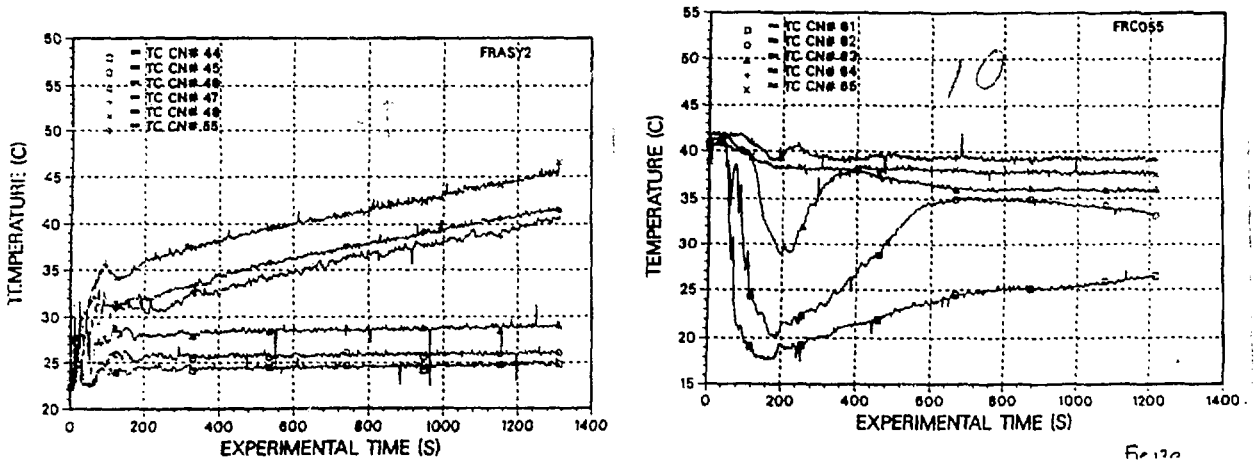

Fig. 10. Severe cold shock to hot pool transient test (C-05) TC data from hot pool vertical sting at 0-degree position.

5. Summary

Construction and operation of complete water test models of the GE PRISM and AI/SAFR ALMR concepts involving many challenging control functions were successfully completed. Results of tests performed to date show that the thermal-hydraulic performance of the PRISM and SAFR concepts are excellent for a wide range of expected operating conditions and thermal shocks to components during transients are mild. The results confirm the analysis assumptions made in the design and no unusual or unexpected phenomenon that affect core coolability was discovered. Thermal stratification was measured in the lower part of the cold pool during thermal up-ramp transients while other portions of the hot and cold pools were well mixed. The potential effect of the stratification on structures in the prototype have not been evaluated but are expected to be negligible because of the relatively infrequent occurrent of thermal up-ramps to the cold pool.

In the SAFR model asymmetric thermal behavior in both the natural convection tests and N-1 loop operation was observed and warrants additional attention.

6. Acknowlegement

Work supported by the U.S. Department of Energy, Office of Reactor Systems Technology under Contract W-31-109-Eng-38.